

# An experimental and modeling study of the contribution of coal ash to SO<sub>2</sub> capture in fluidized bed combustion

Borislav Grubor<sup>a,\*</sup>, Vasilije Manovic<sup>b</sup>, Simeon Oka<sup>a</sup>

<sup>a</sup> Institute for Nuclear Sciences Vinca, P.O. Box 522, 11001 Belgrade, Serbia and Montenegro

<sup>b</sup> Mining and Geology Faculty, Belgrade University, Djusina 7, 11000 Belgrade, Serbia and Montenegro

## Abstract

The process of sulfur self-retention (SSR) occurs as a result of the reactions between the mineral matter in coal ash and the SO<sub>2</sub> evolved during coal combustion. Consequently, the emission of SO<sub>2</sub> may be significantly reduced. The results of experimental investigations and modeling of SSR is presented in this work. The transformations of sulfur forms during devolatilization are taken into account via a correlation for the amount of sulfur that remains in the char, after devolatilization. A novel approach has been applied for modeling SSR during char combustion, closely related to the grain model used for SO<sub>2</sub> retention by limestone as a sorbent. It is assumed that SSR is a result of the reaction between SO<sub>2</sub> and CaO in the form of uniformly distributed micro-grains in char. An unreacted shrinking core model is adopted for the reactions between the CaO micro-grains and SO<sub>2</sub>. The comparison with the experimentally obtained values in a fluidized bed reactor and in a laboratory oven, using coals of different rank (fixed carbon over volatile matter ratio,  $C_{\text{fix}}/\text{VM} = 0.75\text{--}7.40$ ), content of sulfur forms (total 0.84–6.04%, organic 0.71–4.71%, pyritic 0–2.57%) and molar Ca/S ratio (0.34–3.17), has shown that the model can adequately predict the kinetics of the process, the levels of the obtained values of SSR efficiencies, as well as the influence of temperature, coal particle size and the surrounding conditions.

© 2003 Elsevier B.V. All rights reserved.

*Keywords:* Coal combustion; Sulfur retention by ash; Modeling

## 1. Introduction

In the course of development of fluidized bed combustion (FBC) boilers for domestic coals, in the Laboratory for Thermal Engineering and Energy of the Institute for Nuclear Sciences Vinca, special attention was paid to the fundamental research on single coal particle behavior in fluidized bed, in order to reveal the influence of coal characteristics on boiler concept and design. These investigations [1,2], which started from 1976, encompassed the processes of bed to coal particle heat and mass transfer, kinetics of devolatilization, particle fragmentation, ignition temperature and start-up temperature and combustion kinetics of coal and char. The experimental research was supported by mathematical modeling of the particle heating and particle temperature distribution and history, particle fragmentation and char combustion.

Initially, investigations in our Laboratory in relation to sulfur retention were limited to experimental characterization of domestic limestones with the aim of determining the influence of the limestone type, particle size, temperature

and SO<sub>2</sub> concentration on the degree of sulfation [3]. In due course, when a number of stationary FBC combustion tests showed that in the case of some coals substantial sulfur retention can be achieved without the addition of limestone, our interest for the process of sulfur self-retention (SSR) by coal ash itself was enhanced. This new orientation is also in accordance with our opinion, that processes in and around coal particle are crucial for FBC boiler design and overall behavior. Investigation of sulfur self-retention completes our fundamental interest in coal particle behavior under FBC conditions.

Also, the numerous investigations of SSR under FBC conditions by other authors [4–7] have shown that a substantial part of sulfur may be retained in the ash, decreasing the needed amount of limestone to be added. Puff et al. [4] reported that around 60% of sulfur is retained due to SSR, while values near 90% were obtained with fly ash recirculation or combustion of coal rich with tailings.

In our earlier investigations [8] no direct correlation could be found between the molar Ca/S ratio in coal and the amount of sulfur retained in the ash and this fact initiated further investigations in order to determine the influence of coal characteristics and combustion conditions on the SSR process. The results of the recent experimental investigations

\* Corresponding author. Tel.: +381-11-455695; fax: +381-11-453670.  
E-mail addresses: grub@vin.bg.ac.yu, ite@vin.bg.ac.yu (B. Grubor).

## Nomenclature

$A_D$	pre-exponential factor for ionic diffusion of CaO through CaSO <sub>4</sub> (m <sup>2</sup> /s)
$A_i$	pre-exponential factor for $i$ -chemical reaction, 1st (mol/m <sup>2</sup> s), 2nd (mol/m <sup>3</sup> s)
$A_s, A_d$	pre-exponential factor for sulfation and decomposition reaction (m <sup>4</sup> /mol s) (mol/m <sup>2</sup> s)
$c_j$	concentration of $j$ -component (a—ambient, s—char particle surface) (mol/m <sup>3</sup> )
$C_{\text{fix}}$	fixed carbon content in coal (% dry coal basis)
$C_{p,j}$	specific heat capacity of $j$ -component (J/mol K)
$C_{p,v}$	specific heat capacity of porous char particle (J/m <sup>3</sup> K)
$D_{\text{CaO}}$	ionic diffusion coefficient of CaO through CaSO <sub>4</sub> (m <sup>2</sup> /s)
$D_{\text{eff}}$	effective gas diffusion coefficient (m <sup>2</sup> /s)
$E$	activation energy (J/mol)
$E_D$	activation energy for ionic diffusion of CaO through CaSO <sub>4</sub> (J/mol)
$k_m$	mass transfer coefficient between char particle and its surrounding (m/s)
$k_s, k_d$	reaction rate constant for sulfation and decomposition (m <sup>4</sup> /mol s) (mol/m <sup>2</sup> s)
$M_j$	molar mass of $j$ -component (kg/mol)
$N_j$	molar flux of $j$ -component (mol/m <sup>2</sup> s)
$r, R$	current radius and particle radius (m)
$r_c$	unreacted core radius of CaO grain (m)
$R_g$	universal gas constant (J/mol K)
$\mathfrak{R}$	reaction rate (mol/m <sup>3</sup> s)
$S_{\text{Ash}}$	sulfur content in ash (% on dry coal basis)
$S_G$	specific surface of micro-grains (m <sup>2</sup> of CaO micro-grains/m <sup>3</sup> of char)
$S_{\text{CCh}}$	combustible sulfur content in char ( $S_{\text{CCh}} = S_{\text{TCh}} - S_S$ ) (% dry coal basis)
$S_{\text{TCh}}$	total sulfur content in char (% dry coal basis)
$S_O$	organic sulfur content in coal (% dry coal basis)
$S_P$	pyritic sulfur content in coal (% dry coal basis)
$S_{\text{por}}$	specific surface area of porous char particle (m <sup>2</sup> /m <sup>3</sup> )
$S_S$	sulfate sulfur content in coal (% dry coal basis)
$S_T$	total sulfur content in coal (% dry coal basis)
$T$	temperature (a—ambient, s—char particle surface) (K)
VM	volatile matter content in coal (% dry coal basis)
$x_j, X_j$	local and total conversion of $j$ -component (–)
$Y_{\text{CaO}}$	mass fraction of CaO in char (–)

## Greek letters

$\alpha$	convective heat transfer coefficient between char particle and ambient (W/m <sup>2</sup> K)
$\varepsilon$	char particle porosity (–)
$\varepsilon_r$	emissivity (–)
$\eta_{\text{SO}_2}$	sulfur self-retention efficiency ( $\eta_{\text{SO}_2} = S_{\text{Ash}}/S_T \times 100$ ) (%)
$\lambda_{\text{eff}}$	effective heat conductivity of porous char particle (W/m K)
$\nu_{i,j}$	stoichiometric coefficients for $i$ -reaction and $j$ -component (–)
$\rho$	density (kg/m <sup>3</sup> )
$\sigma$	Stefan–Boltzman constant (W/m <sup>2</sup> K <sup>4</sup> )
$\tau$	time (s)
$\chi_{\text{O}_2}$	molar fraction of O <sub>2</sub> (–)

## Subscripts

0	initial value
1, 2	combustion reactions 1 and 2
Ch	char particle
d	decomposition of CaSO <sub>4</sub>
f	formation of SO <sub>2</sub> due to combustion
G	CaO grain
s	sulfation

as well as the developed overall model for the SSR process, taking into account both devolatilization and char combustion, are presented in this paper. A novel approach has been applied for modeling SSR during char combustion, closely related to the grain model [9–11] used for the SO<sub>2</sub> retention by limestone addition.

## 2. Reactions and redistribution of sulfur during coal combustion

The mechanism of gaseous sulfur compounds formation and their subsequent reactions significantly differ during devolatilization and char combustion. According to Attar [12], the reactions of sulfur compounds that occur inside the coal particle during devolatilization can be categorized as follows: reactions of pyrites, reactions of organic sulfur and reactions between mineral matter and sulfur compounds.

Pyrite decomposes during devolatilization according to the following reaction:  $\text{FeS}_2 \rightarrow \text{FeS} + \text{S}$ , which starts around 550–600 °C. In the temperature range 700–1000 °C, the final product of pyrite decomposition remaining in the char is FeS, regardless of coal rank and devolatilization conditions [13].

Generally speaking, the content of various organic functional groups containing sulfur depends on the coal rank. The results of the investigation of the distribution of organic sulfur groups show that the content of non-thiophenic sulfur decreases while the content of thiophenes increases with coal rank [13–15]. This is explained by the fact that stable thiophenes are formed from less stable organic sulfur compounds (thiols and sulfides), during carbonification [16]. In other words, it may be said that coals of similar rank have a similar distribution of sulfur-containing functional groups. Calkins [17] demonstrated that during devolatilization aliphatic sulfides, mercaptans and disulfides decompose at 600–800 °C, aromatic sulfides and mercaptans at 900 °C, while thiophenic sulfur compounds decompose at even higher temperatures. As a result, mainly thiophenes remain in the char after devolatilization [17,18].

Due to the prevailing reducing conditions during devolatilization, H<sub>2</sub>S is the most common sulfur-containing gaseous compound in the volatiles. Other compounds, like COS and CS<sub>2</sub>, are present to a lesser extent. A certain amount of sulfur, present in the constituents of tar, is released with the tar [19,20]. The most important reaction of H<sub>2</sub>S, which is formed by the decomposition of pyrite and organic compounds, is the reaction with carbonates (predominantly CaCO<sub>3</sub> and MgCO<sub>3</sub>) and oxides formed from them. The final products are sulfides, by which a part of the H<sub>2</sub>S is retained in the char [21].

The sulfur compounds released during devolatilization are subsequently oxidized to SO<sub>2</sub>. This oxidation occurs during the combustion of the volatiles and takes place outside the parent coal particle. The amount of sulfur that is released during devolatilization of coal largely depends on the coal

sulfur content, forms of sulfur and, to a lesser extent, on other coal properties and devolatilization conditions. With increasing devolatilization temperature, the amount of sulfur remaining in the char decreases, but not significantly in the temperature range 700–1000 °C [13,19,20]. Thus, in this temperature range, the coal characteristics and content of sulfur forms in coal have a predominant influence on the amount of sulfur that remains in the char [22].

Several attempts have been made toward formulating correlations for estimating the sulfur content in the char after devolatilization. These correlations are either presented graphically [23] or as explicit equations resulting from fitting the experimental data [24]. Attempts have also been made to model the reactions of sulfur compounds during devolatilization [20,25].

Contrary to the oxidation of sulfur released during devolatilization, the oxidation of sulfur during char combustion takes place inside the char particle. The formed SO<sub>2</sub> diffuses outwards through the char particle pores during which a part of SO<sub>2</sub> may react with the base oxides forming sulfates that remain in the ash. Thus, most of the SSR by ash occurs during char combustion. The most important base oxide for SSR is CaO, formed as a result of CaCO<sub>3</sub> decomposition and combustion of organic groups containing Ca [26]. A direct correlation between the molar Ca/S ratio of coal and the SSR efficiency has not yet been established (even under similar combustion conditions). This may be a consequence of the different degree of dispersion and reactivity of calcium, as well as the contribution of other base oxides (MgO, K<sub>2</sub>O, Na<sub>2</sub>O) [6,27–31]. Sheng et al. [27,28] considered that the very active Ca is bound within the coal matrix as exchangeable ions, and concluded that the activity of Ca increases as the rank of coal decreases. The same authors reported that, under FBC conditions, other base oxides are significantly less reactive than CaO. Conn et al. [31] investigated the reactivity of various Ca forms in low-rank coals and state that the calcium present in clays and silicates cannot react with SO<sub>2</sub> under FBC conditions.

The heterogeneous reaction of SO<sub>2</sub> with CaO (termed sulfation) is first order with respect to SO<sub>2</sub> and zero order with respect to O<sub>2</sub> [32]. The final product of sulfation is the solid CaSO<sub>4</sub>, which remains in the ash. The sulfation reaction has been mostly investigated in the case of SO<sub>2</sub> retention by CaCO<sub>3</sub> as a sorbent [33,34]. This process is mostly used in the case of FBC combustion of coal since it enables sulfation to take place in the optimum temperature range (800–900 °C). There are numerous expressions for sulfation kinetics in the literature, ranging from empirical ones [35] up to expressions of the Arrhenius type [36]. Kinetic parameters (pre-exponential factor and activation energy) differ significantly, depending on the physical model used. The basic difference between the various models of sulfation is whether the formation of a solid product layer of CaSO<sub>4</sub>, as well as diffusion through this layer [37,38], is taken into account. In that case the sulfation rate is diffusion limited [39].

There is sufficient experimental evidence that the degree of CaO conversion goes through a maximum as the temperature increases [7,9]. There are different explanations for this phenomenon in the literature: thermal [32] or reductive (due to the higher CO concentrations) [40] decomposition of CaSO<sub>4</sub>. Also, sintering may occur at higher temperatures [41] due to which the exposed surface of the CaO decreases, thus hindering the process of sulfation.

Only a few models of the SSR process [7,25] or correlations [24,42] for estimating sulfur content in the ash after combustion can be found in the literature, but their wider applicability has not yet been proven. In the existing models of SSR the sulfation rate is taken into account in a simplified manner, disregarding the decrease of the reaction rate due to diffusion through the product layer. Yeh et al. [7] take the char pore surface area as a measure of the available surface of CaO for sulfation reaction, while Chen and Kojima [25] take into account the concentration of CaO in the coal briquette.

### 3. Experimental

Since the data on SSR is relatively scarce in the literature, an experimental program was designed in order to study this phenomenon in greater detail and to determine the influence of coal rank, content of sulfur forms, molar Ca/S ratio, coal particle size, temperature and other surrounding conditions. This program consisted of various experiments with the aim of obtaining data on the amount of sulfur that remains in the char after devolatilization as well as in the ash after combustion. Since it was concluded that the surrounding conditions do not significantly influence the fate of sulfur during devolatilization (in the FBC temperature range), the char samples were obtained in a laboratory oven according to the Yugoslav standard for determination of volatiles yield in coal. In order to study the effect of the surrounding conditions on the amount of sulfur that remains in the ash after combustion, the coal combustion experiments were conducted both in a laboratory oven as well as in an FBC reactor.

#### 3.1. Analysis

The contents of various sulfur forms in the coal, char and ash samples were determined according to the Yugoslav standards. The total sulfur content in both coal and char was determined by combusting the samples in Eschka mixture and subsequently extracting and gravimetrically measuring the sulfates. The sulfate sulfur in the coal and char samples was determined by extracting the sulfates with dilute hot HCl and then measuring them gravimetrically. The pyritic sulfur in the coal was determined indirectly by determining the content of pyritic Fe in the samples, utilizing the fact that pyrite is non-soluble in dilute hot HCl solution, but is soluble in dilute hot HNO<sub>3</sub> solution. The content of organic sulfur in the coal was obtained as the difference between the total and the inorganic sulfur. The sulfur content in the ash was determined by the oxidation of all sulfur compounds to sulfates in hot HCl solution, and then measuring them gravimetrically.

#### 3.2. Experimental procedures

The char samples were obtained in a laboratory furnace at 900 °C. The coal samples (2 g), ground to a particle size less than 0.2 mm, were placed in a pre-heated laboratory furnace in covered ceramic receptacles. In this way the volatile products surrounded the coal particles during devolatilization and thus they did not undergo any significant temperature rise due to combustion of the volatiles, which occurs outside the receptacles.

The experiments were done for six Serbian coals whose characteristics and the obtained results for the sulfur content in their chars are given in Table 1. The chosen coals cover a wide range of rank, from lignites up to a semi-anthracite. It can be seen that 46–75% of the total sulfur remains in the char after devolatilization and these values cannot be correlated with the molar Ca/S ratio. More importantly, the amount of sulfate sulfur in the char is never greater than the amount of sulfate sulfur in the coal, which implies that

Table 1  
Coal characteristics and sulfur content in the obtained char samples<sup>a</sup>

	Kolubara (lignite)	Kostolac (lignite)	Soko (brown coal)	Bogovina (brown coal)	Ibar (hard coal)	V. Cuka (semi-anthracite)
Moisture (%)	13.66	12.91	8.44	6.58	1.22	1.47
Ash (%)	16.34	22.76	12.06	19.75	34.37	24.16
VM (%)	47.69	40.61	41.79	39.21	23.01	9.03
C <sub>fix</sub> (%)	35.97	36.63	46.16	41.04	42.62	66.81
LHV (kJ/g)	15.14	13.26	20.37	15.76	16.66	23.18
Ca/S	2.95	1.60	0.81	1.09	0.34	3.17
S <sub>S</sub> (%)	0.11	0.31	0.09	0.22	0.62	0.11
S <sub>P</sub> (%)	0.00	0.24	0.23	0.09	2.57	0.36
S <sub>O</sub> (%)	0.73	1.70	1.84	4.31	2.85	0.71
S <sub>T</sub> (%)	0.84	2.25	2.16	4.62	6.04	1.18
S <sub>T</sub> in char (%)	0.53	1.55	1.17	2.49	4.00	0.89
S <sub>S</sub> in char (%)	0.05	0.22	0.06	0.12	0.11	0.06

<sup>a</sup> All values (apart from moisture) given on dry coal basis.

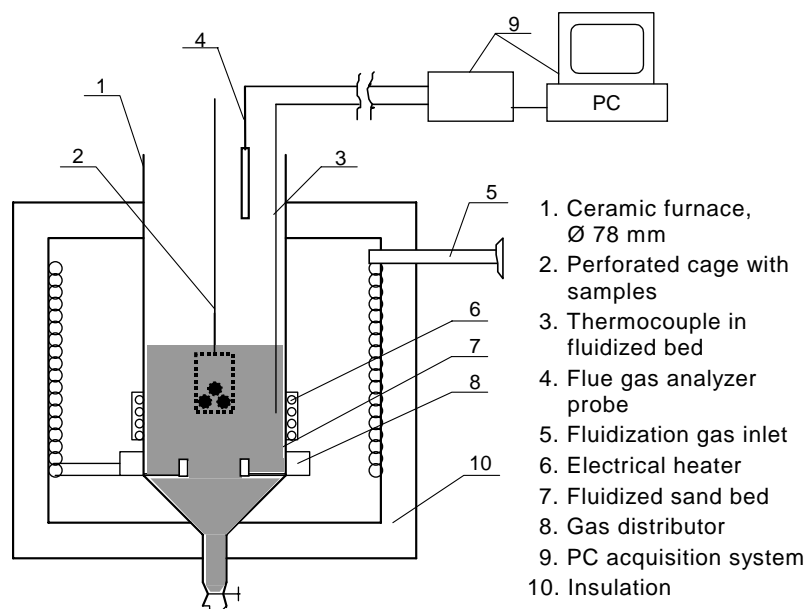


Fig. 1. The schematics of the FBC reactor.

during devolatilization practically no SSR occurs. The major part of the sulfur that remains in the char is combustible and a part of it may be retained in the ash only during char combustion.

The experiments with the aim of obtaining the amount of sulfur that remains in the ash after combustion were done with coals Kolubara and Bogovina. The batch combustion tests were carried out both in an FBC reactor and in a laboratory oven (both pre-heated up to the desired temperature level). The experiments were done with three particle size fractions (4.0–7.0, 7.0–10 and 10–13 mm) and at three surrounding temperatures (750, 800 and 850 °C). The SSR efficiency in all cases was determined taking into account the total sulfur content in the coal and in the ash:  $\eta_{SO_2} = S_{Ash}/S_T \times 100$ .

The main part of the FBC reactor facility, shown in Fig. 1, is made of a Ø78 mm ceramic tube. Silica sand particles of 0.5 mm were used as the inert bed material while the fixed bed height was 60 mm. The bed was fluidized by air (fluidization number in the range of 2.0–2.5) and heated up with electrical heaters that surround the ceramic tube. The coal batches were placed inside a perforated cage and the batch mass for each sample was chosen such that the bed temperature would not change more than 5 °C due to coal combustion. Each experimental run was performed with fresh sand in order to eliminate possible contamination with coal ash from the previous run that could affect the SO<sub>2</sub> retention in the subsequent run. During the tests the SO<sub>2</sub> concentrations on the top of the bed were monitored in the freeboard, close to the bed surface. The data on SSR, obtained both in the laboratory oven and in the FBC reactor, will be analyzed in the course of comparison with the model predictions.

#### 4. Sulfur self-retention model description

The scope and the main characteristics of the model that is presented are as follows:

- Since it was concluded that SSR does not occur during devolatilization, an attempt was made to define a correlation for estimation of the amount of sulfur that remains in the char, after devolatilization.
- In order to determine the conditions and parameters relevant for the SSR during char combustion, a previously developed model of combustion was adopted [43,44]. This model belongs to the group of microscopic models of intrinsic reactivity and describes the dynamic behavior of a porous char particle during combustion. The processes of fragmentation and attrition are neglected, i.e. the char particle radius remains constant. The process of combustion occurs in a relatively narrow, inward moving front and is predominantly controlled by oxygen diffusion through the formed outer ash layer.
- It is assumed that the main contribution to SSR is the sulfation reaction between the SO<sub>2</sub> and the CaO in the char. This occurs in the ash layer through which the SO<sub>2</sub> diffuses outward and in which there is sufficient oxygen for the sulfation reaction to proceed.
- A novel approach has been applied concerning the form in which the CaO is present in the char, i.e. it is assumed that all of the active Ca is present in the form of the CaO micro-grains (Fig. 2). This approach is closely related to the grain model [11] used for the SO<sub>2</sub> retention by limestone addition. The decomposition of the formed CaSO<sub>4</sub> at higher temperatures is taken into account by a reaction whose kinetics is of the Arrhenius type.

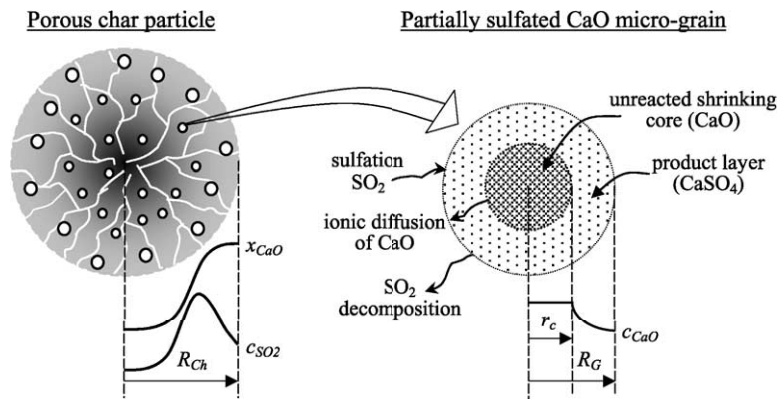


Fig. 2. Schematic representation of a burning porous char particle and a partially sulfated CaO micro-grain.

Taking into account the behavior of various sulfur forms during devolatilization, the following assumptions were considered in formulating a correlation for the total sulfur content in the char, after devolatilization:

1. The total amount of sulfate sulfur in the coal remains in the char. This assumption is not quite correct since usually the sulfate sulfur content in the char is somewhat smaller than in the coal (Table 1), but the amount of sulfate sulfur is sufficiently small to justify the stated assumption.
2. One half of the pyritic sulfur (in the form of FeS) remains in the char as a result of decomposition of pyrite according to the following reaction:  $\text{FeS}_2 \rightarrow \text{FeS} + \text{S}$ .
3. The organic sulfur content in the char is proportional to the organic sulfur content in the coal. The proportionality coefficient can be defined as equal to  $C_{\text{fix}}/(C_{\text{fix}} + \text{VM})$ , implying that the organic sulfur is evenly distributed in the coal combustible matter, i.e. both in the volatiles and the  $C_{\text{fix}}$ .

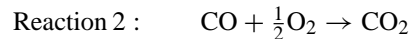
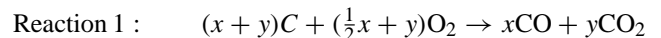
A certain drawback of the second and third assumption is the disregard of the fact that part of the sulfur formed by the decomposition of pyrite reacts with the organic substance and stays in the char. Also, part of the  $\text{H}_2\text{S}$  formed by the decomposition of organic substance or derived from pyrite, may react with the base oxides and in this way remain in the char. The quantitative effects of these reactions are difficult to evaluate and even more so to incorporate into a simplified correlation.

Based on the previous assumptions, the following correlation may be derived for evaluating the total sulfur content

in the char ( $S_{\text{TCh}}$ ), after devolatilization:

$$S_{\text{TCh}} = 0.5S_{\text{P}} + \frac{C_{\text{fix}}}{C_{\text{fix}} + \text{VM}} S_{\text{O}} + S_{\text{S}} \quad (1)$$

The previously developed model for char combustion [43,44] is adopted as a basis for the SSR model, and thus only the main features will be outlined. It is assumed that the main reactions are



Reaction 1 is a heterogeneous reaction of oxidation of solid carbon that takes place both on the surface of the pores and on the surface of the char particle, while reaction 2 is a homogenous reaction of oxidation of CO that takes place inside the pores and its rates are defined as

$$\mathfrak{R}_1 = \frac{dc_{\text{C}}}{d\tau} = -A_1 \chi_{\text{O}_2} \exp\left(\frac{-E_1}{R_{\text{g}}T}\right) S_{\text{por}} \quad (2)$$

$$\mathfrak{R}_2 = \frac{dc_{\text{CO}}}{d\tau} = -A_2 c_{\text{CO}} c_{\text{O}_2}^{0.5} c_{\text{H}_2\text{O}}^{0.5} \exp\left(\frac{-E_2}{R_{\text{g}}T}\right) \varepsilon \quad (3)$$

$$\gamma = \frac{x}{y} = \frac{c_{\text{CO}}}{c_{\text{CO}_2}} = 2512 \exp\left(\frac{-51880}{R_{\text{g}}T}\right) \quad (4)$$

where Eq. (4) defines the primary molar CO/CO<sub>2</sub> ratio in reaction 1. The values of all kinetic parameters are given in Table 2.

The main mechanism of heat transfer inside the char particle is conduction and radiation while mass transfer is

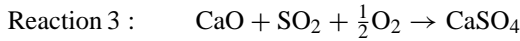
Table 2  
Kinetic parameters used in the model

Reaction	Pre-exponential factor	Activation energy	Source
Reaction 1 (Eq. (2))	$A_1 = 254.16 \text{ mol/m}^2 \text{ s}$	$E_1 = 179.4 \text{ kJ/mol}$	[47]
Reaction 2 (Eq. (3))	$A_2 = \text{model parameter}^a$	$E_2 = 55.695 \text{ kJ/mol}$	[48]
Sulfation (Eq. (6))	$A_s = 2.2 \times 10^{-3} \text{ m}^4/\text{mol s}$	$E_s = 61.5 \text{ kJ/mol}$	[11]
Decomposition (Eq. (7))	$A_d = 5.0 \times 10^7 \text{ mol/m}^2 \text{ s}$	$E_d = 300.00 \text{ kJ/mol}$	Used in this work

<sup>a</sup> Fitting parameter according to our own experimental data on char combustion [44].

achieved by molecular diffusion, taking into account porosity and pore tortuosity. The char combustion model enables prediction of spatial and temporal changes of all important physical properties (porosity, internal specific surface area, thermal conductivity) and parameters (temperature, gas concentrations, effective diffusivity, conversion degree).

It is assumed that  $\text{SO}_2$  is the only product of combustion of sulfur compounds, which diffuses outward from the combustion front and reacts with the  $\text{CaO}$  in the outer ash layer forming  $\text{CaSO}_4$  according to the following sulfation reaction:



The active part of  $\text{CaO}$  in coal is formed as a result of  $\text{CaCO}_3$  decomposition and combustion of the Ca-containing organic compounds. As stated before, the calcium present in clays and silicates cannot react with  $\text{SO}_2$  under FBC conditions. The procedure for the evaluation of the active part of  $\text{CaO}$  is presented in [26]. It is assumed that after devolatilization all of the active Ca is present in the form of  $\text{CaO}$  micro-grains of the same initial radius ( $R_{G,0}$ ), which are uniformly distributed throughout the char volume.

The rates of  $\text{SO}_2$  formation (assumed to be proportional to the rate of carbon conversion), sulfation and  $\text{CaSO}_4$  decomposition are defined by the following expressions (the kinetic parameters given in Table 2):

$$\mathfrak{R}_f = \frac{\partial c_{\text{SO}_2, f}}{\partial \tau} = -\mathfrak{R}_1 \frac{S_{\text{CCh}}}{C_{\text{fix}}} \frac{M_{\text{C}}}{M_{\text{S}}} \quad (5)$$

$$\mathfrak{R}_s = \frac{\partial c_{\text{SO}_2, s}}{\partial \tau} = -k_s S_G c_{\text{CaO}} c_{\text{SO}_2},$$

$$\text{where } k_s = A_s \exp\left(\frac{-E_s}{R_g T}\right) \quad (6)$$

$$\mathfrak{R}_d = \frac{\partial c_{\text{SO}_2, d}}{\partial \tau} = k_d S_G, \quad \text{where } k_d = A_d \exp\left(\frac{-E_d}{R_g T}\right) \quad (7)$$

The sulfation reaction, whose rate is zero order with respect to  $\text{O}_2$ , may proceed only if there is sufficient oxygen according to reaction 3. This means that no sulfation occurs in the region inward from the combustion front. In parallel to the sulfation a process of decomposition of the formed  $\text{CaSO}_4$  takes place, which is treated here in a simplified manner by Eq. (7), i.e. its rate is taken to depend only on temperature and specific surface. The aim is to obtain a temperature maximum in the SSR efficiency, without considering the true mechanisms by which this decomposition occurs. At this time, the mechanisms of the  $\text{CaSO}_4$  decomposition process are not fully understood, nor is there agreement on the origin of the well-known sulfur-capture efficiency temperature maximum [33].

An unreacted shrinking core model is adopted for the reactions between the  $\text{CaO}$  micro-grains and  $\text{SO}_2$ . A partially sulfated  $\text{CaO}$  micro-grain is shown in Fig. 2. It consists of the unreacted shrinking core, of radius  $r_c$ , surrounded by a

product layer of  $\text{CaSO}_4$ . As the process of sulfation progresses, the size of the grains increases ( $R_G > R_{G,0}$ ) due to the larger molar volume of  $\text{CaSO}_4$  in comparison to  $\text{CaO}$ . It is assumed that the  $\text{Ca}^{2+}$  ions migrate outward (and  $\text{O}^{2-}$  in a coupled manner to satisfy local mass and charge balances) through the product layer. This type of product layer diffusion, which may occur by various mechanisms such as interstitial or vacancy, was proposed by Hsia et al. [45,46] based on their experimental investigations. This approach was used by Mahuli et al. [11] for modeling the  $\text{CaO-SO}_2$  reaction.

Taking into account the content of Ca in the char particle, the  $\text{CaO}$  micro-grain dimensions and the properties of the char particle, the specific surface for the reactions of sulfation and decomposition is derived as

$$S_G = 3Y_{\text{CaO}} \frac{\rho_{\text{Ch},0}}{\rho_{\text{G},0}} \frac{R_G^2}{R_{G,0}^3} \quad (8)$$

The  $\text{CaO}$  concentration ( $c_{\text{CaO}}$ ) in Eq. (6) is related to the surface of the  $\text{CaO}$  micro-grains and is determined by the pseudo-steady-state condition

$$\frac{\partial}{\partial r} \left( r^2 \frac{\partial c_{\text{CaO}}}{\partial r} \right) = 0 \quad (9)$$

with the following boundary conditions:

$$c_{\text{CaO}}|_{r=r_c} = \frac{\rho_{\text{G},0}}{M_{\text{CaO}}} \quad \text{and} \\ -D_{\text{CaO}} \left( \frac{\partial c_{\text{CaO}}}{\partial r} \right) \Big|_{r=R_G} = k_s c_{\text{CaO}} c_{\text{SO}_2} - k_d$$

The solution of the partial differential equation (9) gives the  $\text{CaO}$  concentration profile in the product layer of the reacting  $\text{CaO}$  micro-grain (Fig. 2). At the micro-grain surface the  $\text{CaO}$  concentration is

$$c_{\text{CaO}} = \frac{(\rho_{\text{G},0}/M_{\text{CaO}})D_{\text{CaO}} + R_G k_d (R_G/r_c - 1)}{D_{\text{CaO}} + R_G k_s c_{\text{SO}_2} (R_G/r_c - 1)} \quad (10)$$

The ionic diffusion coefficient through the product layer is of the Arrhenius type

$$D_{\text{CaO}} = A_D \exp\left(\frac{-E_D}{R_g T}\right) \quad (11)$$

The change of the unreacted core radius is obtained by solving the following differential equation that takes into account the net effect of sulfation and decomposition:

$$\frac{dr_c}{d\tau} = \frac{M_{\text{CaO}}}{\rho_{\text{G},0}} \frac{R_G^2}{r_c^2} (k_d - k_s c_{\text{CaO}} c_{\text{SO}_2}) \quad (12)$$

The determined values of  $r_c$  enable the calculation of the local and overall degree of  $\text{CaO}$  conversion and, in turn, the radius of the partially sulfated  $\text{CaO}$  micro-grains in each char particle segment

$$x_{\text{CaO}} = 1 - \frac{r_c^3}{R_{G,0}^3} \quad \text{and} \quad X_{\text{CaO}} = \frac{3 \int_0^{R_{\text{Ch}}} x_{\text{CaO}}(r) r^2 dr}{R_{\text{Ch}}^3} \quad (13)$$

$$R_G^3 = r_c^3 + z x_{\text{CaO}} R_{G,0}^3 \quad (14)$$

where  $z$  represents the molar volume ratio of  $\text{CaSO}_4$  and  $\text{CaO}$  ( $z = 3.09$ ).

The heat and mass balance, which determine the temperature and concentration profiles of the gaseous compounds ( $\text{O}_2$ ,  $\text{CO}_2$ ,  $\text{CO}$ ,  $\text{SO}_2$ ) along the char particle radius, is described by the following partial differential equations:

$$C_{p,v} \frac{\partial T}{\partial \tau} = \frac{1}{r^2} \frac{\partial}{\partial r} \left( r^2 \lambda_{\text{eff}} \frac{\partial T}{\partial r} \right) + \sum (C_{p,j} N_j) \frac{\partial T}{\partial r} + \Delta H_1 \mathfrak{R}_1 + \Delta H_2 \mathfrak{R}_2 + \Delta H_3 \mathfrak{R}_3 \quad (15)$$

$$\frac{\partial c_j}{\partial \tau} = \frac{1}{r^2} \frac{\partial}{\partial r} \left( r^2 D_{\text{eff}} \frac{\partial c_j}{\partial r} \right) + v_{1,j} \mathfrak{R}_1 + v_{2,j} \mathfrak{R}_2 + v_{3,j} \mathfrak{R}_3 \quad (16)$$

where  $j = 1, 2, 3$  and 4 ( $\text{O}_2$ —1,  $\text{CO}_2$ —2,  $\text{CO}$ —3,  $\text{SO}_2$ —4). The last terms in both of these equations represent the net effect of the  $\text{SO}_2$  formation, sulfation and  $\text{CaSO}_4$  decomposition on the heat and mass balance ( $\Delta H_3 \mathfrak{R}_3 = \Delta H_f \mathfrak{R}_f + \Delta H_s \mathfrak{R}_s + \Delta H_d \mathfrak{R}_d$  and  $v_{3,j} \mathfrak{R}_3 = v_{f,j} \mathfrak{R}_f + v_{s,j} \mathfrak{R}_s + v_{d,j} \mathfrak{R}_d$ ). The following relations define the boundary conditions:

$$r = 0 \Rightarrow \frac{\partial c_j}{\partial r} = 0, \quad \frac{\partial T}{\partial r} = 0$$

$$r = R_{\text{Ch}} \Rightarrow -\lambda \left. \frac{\partial T}{\partial r} \right|^- = \alpha (T_s - T_a) + \frac{(1 - \varepsilon) \Delta H_1 \mathfrak{R}_1}{S_{\text{por}}} + \sigma \varepsilon_r (T_s^4 - T_a^4) \quad \text{and} \\ -D_{\text{eff},j} \left. \frac{\partial c_j}{\partial r} \right|^- = k_m (c_{j,s} - c_{j,a}) + \frac{v_{1,j} \mathfrak{R}_1 (1 - \varepsilon)}{S_{\text{por}}}$$

The expressions used to define the heat and mass transfer between the burning char particle and its surrounding, the change of specific surface area and porosity, the effective gas diffusion coefficient and the effective heat conductivity of the porous char particle are given in [44]. The solution procedure begins with evaluating the total sulfur content in the char, after devolatilization, using Eq. (1). All other initial char properties, relevant to char combustion and SSR, are either evaluated from the known coal properties or experimentally determined (porosity, pore size, specific surface area, active part of Ca, etc.). The initial conditions (temperatures and gas concentrations) are based on the presumed values after devolatilization. The evaluation of these initial conditions is not critical, since they affect the calculations only in the first few seconds of char combustion. The values of all parameters are initially constant along the char particle radius.

For numerical purposes, the char particle is subdivided into segments (usually more than 100) of equal volume. At any time  $\tau$ , parameters related to char combustion and SSR for each char particle segment are calculated using Eqs. (2)–(14), based on the current values of temperatures,

gas concentrations and other necessary parameters. Then the system of partial differential equations (15) and (16) are solved, using the numerical method of control volumes [49]. The whole procedure is repeated until all of the carbon in char is consumed.

## 5. Model verification

Since the main new feature of the presented over-all SSR model is the adopted distribution of  $\text{CaO}$  in the form of micro-grains in the char, the sensitivity of the model to the variation of the parameters that determine the kinetics of the process, in relation to this feature, is analyzed in greater detail. The influence of  $k_s$  and  $D_{\text{CaO}}$ , for different values of  $R_{G,0}$ , is shown in Fig. 3. It may be seen that the variation of  $k_s$ , in the range of values reported in the literature

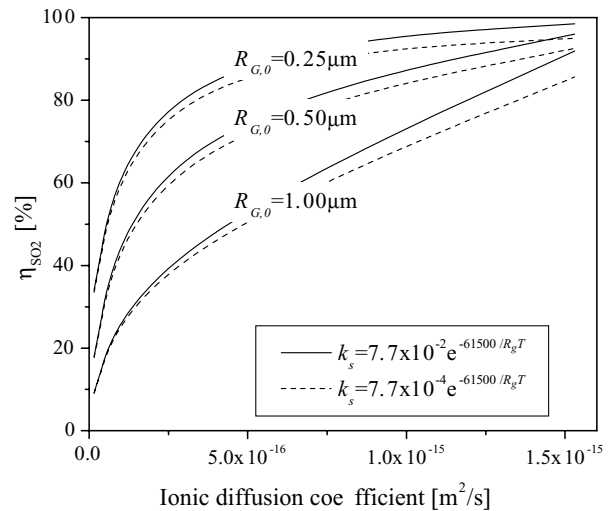


Fig. 3. Sensitivity of the model to the variation of  $k_s$  and  $D_{\text{CaO}}$ .

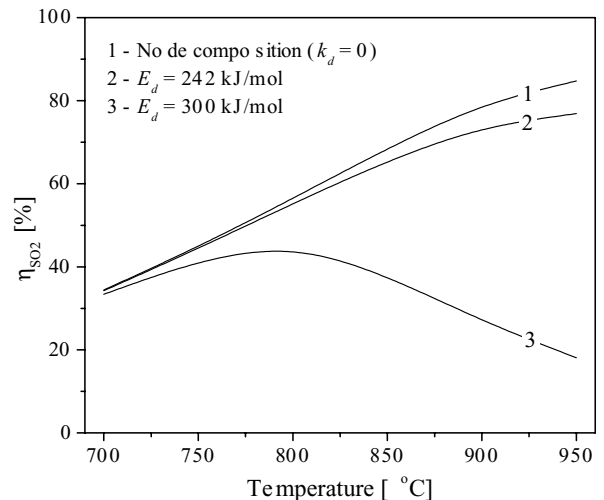


Fig. 4. Sensitivity of the model to the variation of  $E_d$ .



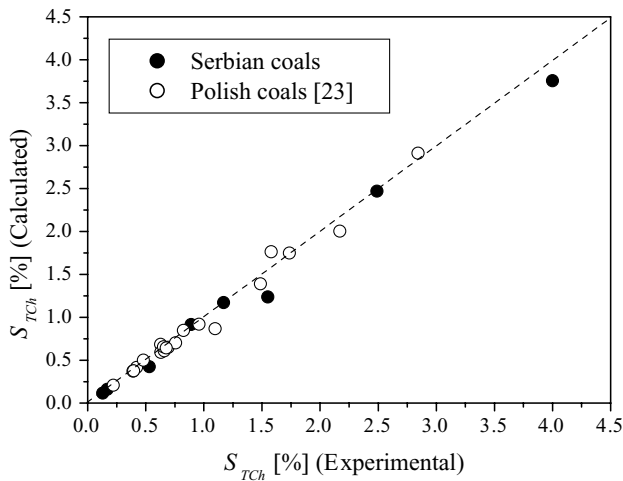


Fig. 5. Experimental and calculated content of total sulfur in char ( $S_{TCh}$ ), according to Eq. (1).

[36,50], does not significantly influence the calculated SSR efficiency. On the other hand, the influence of  $D_{CaO}$  and  $R_{G,0}$  is quite noticeable. This shows that the process of SSR is limited by ionic diffusion through the product layer and that  $D_{CaO}$  and  $R_{G,0}$  are important model parameters whose values should be chosen by comparing model results with experimental data. The presented curves were obtained using the following set of data for the char particle:  $R_{Ch} = 2$  mm,  $C_{fix} = 80\%$ ,  $\varepsilon_0 = 50\%$ ,  $S_{por,0} = 200$  m<sup>2</sup>/cm<sup>3</sup>,  $S_{TCh} = S_{CCh} = 2\%$ ,  $Ca/S = 1$ ,  $T = 800$  °C with air as the fluidizing gas ( $c_{O_2} = 21\%$ ), but similar conclusions were verified using quite different sets of data. For further analysis in this work the following values of these parameters were assumed:  $D_{CaO} = 10^{-10} \exp(-125\,000/R_g T)$ ,  $k_s = 2.2 \times 10^{-3} \exp(-61\,500/R_g T)$  and  $R_{G,0} = 0.5$   $\mu$ m.

The influence of temperature on the SSR efficiency, for different values of  $k_d$  (i.e.  $E_d$ ), is shown in Fig. 4. Under the assumption that there is no decomposition ( $k_d = 0$ ), the SSR

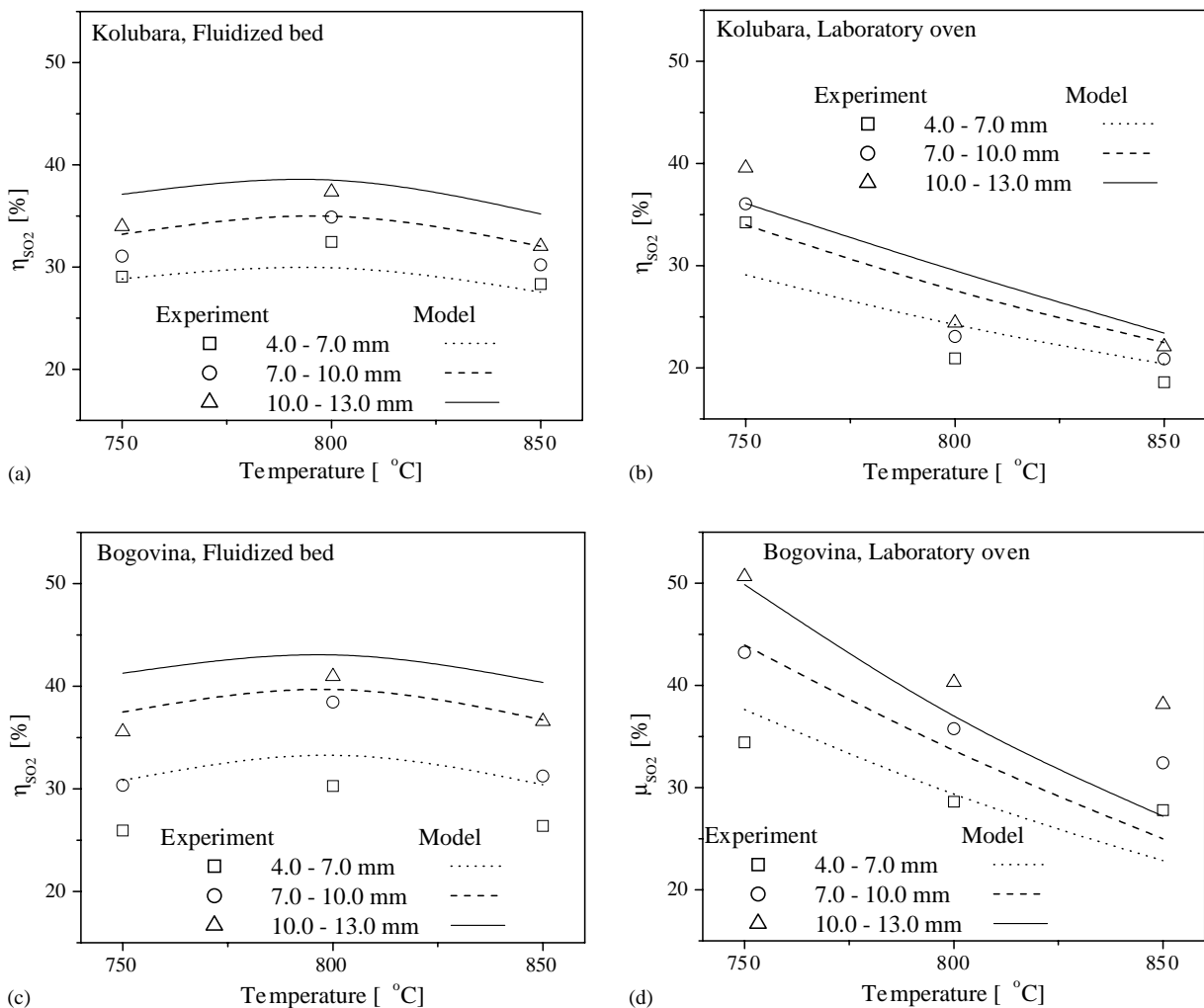


Fig. 6. Experimental values and model predictions of overall sulfur self-retention efficiency for batch combustion of coals Kolubara and Bogovina in FBC reactor and laboratory oven.

Table 3  
Char characteristics and some model parameters

Parameters	Kolubara	Bogovina
$\rho_{\text{Ch},0}$ (kg/m <sup>3</sup> )	850	1140
$\varepsilon_0$ (-)	0.51	0.39
$S_{\text{por},0}$ (m <sup>2</sup> /cm <sup>3</sup> )	190	155
$A_2$ (mol/m <sup>3</sup> s)	$7.43 \times 10^5$	$7.15 \times 10^5$
$A_D$ (m <sup>2</sup> /s)	$1.0 \times 10^{-10}$	$1.0 \times 10^{-10}$
$E_D$ (kJ/mol)	125.0	125.0
$R_{G,0}$ ( $\mu\text{m}$ )	0.50	0.50

efficiency would continually increase with the surrounding temperature (curve 1). This is not in accordance with the available experimental data in the literature that show that there is an optimal temperature after which the SSR efficiency decreases. If the value of  $E_d = 242.0$  kJ/mol is used, a literature value for CaSO<sub>4</sub> reduction due to CO [51], the SSR efficiency maximum would be at much higher temperatures (curve 2) than reported in the literature (around 850 °C in the case of limestone). For further analysis in this work a greater value for  $E_d$  (300 kJ/mol) was chosen which leads to a temperature maximum of around 800 °C (curve 3), in compliance with the majority of data on SSR in the literature, as well as with the experimental data presented in this work.

The results of comparison between the experimentally obtained data (Table 1) as well as the data for 20 Polish coals with quite different properties [23] and the calculated values of the amount of sulfur that remains in the char using Eq. (1) are given in Fig. 5. It may be seen that, regardless of the simplifying assumptions related to Eq. (1), there is quite good agreement between the calculated and experimentally obtained values of  $S_{\text{TCh}}$ .

Model predictions for the overall SSR efficiency are compared with the obtained experimental data in Fig. 6. The input data for model predictions consisted of the coal

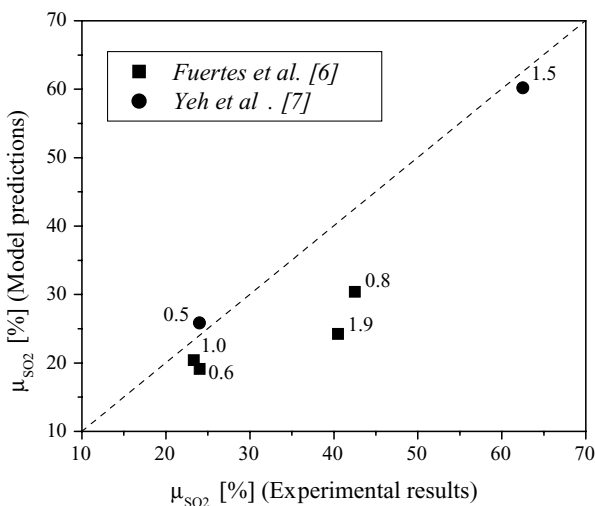


Fig. 7. Experimental values and model predictions of  $\eta_{\text{SO}_2}$  for literature data (numbers close to symbols denote the molar Ca/S ratio).

characteristics (Table 1), kinetic parameters (Table 2) and other char characteristics and model parameters given in Table 3. It may be seen that the model predicts relatively well the levels of the SSR efficiencies, as well as the influence of temperature and particle size. Under the FBC conditions the maximum obtained experimental values of SSR were around 800 °C while in the laboratory oven the SSR decreases with temperature. The same behavior is obtained using the model and can be explained by different temperatures inside the char particles during combustion. For the same surrounding temperature, temperature inside the char particle is higher during combustion in the laboratory oven due to the smaller heat transfer rates between char particles and the ambient. The increase of the SSR levels with the increase of particle size is noticed in all cases and may be explained as a consequence of longer SO<sub>2</sub> diffusion paths. The existence of the SSR temperature maximum under FBC conditions and the beneficial effect of particle size are also reported by other authors [7].

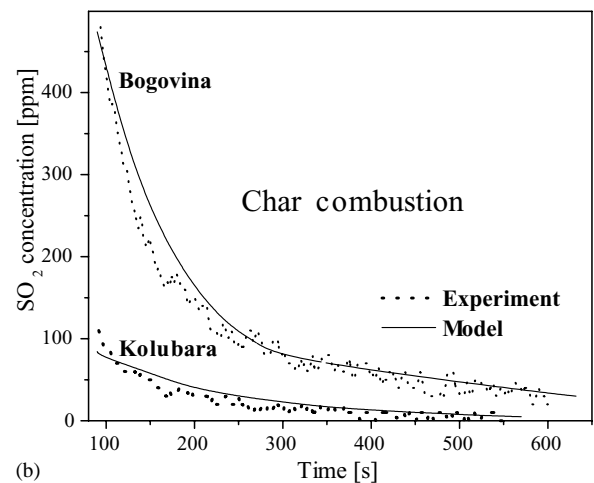
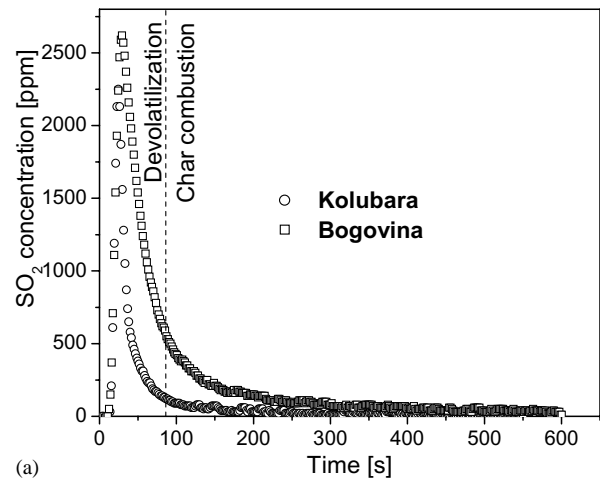


Fig. 8. SO<sub>2</sub> concentration at top of FBC reactor during batch combustion of coal,  $T_{\text{bed}} = 750$  °C,  $R_{\text{Ch}} = 2\text{--}3.5$  mm: (a) experimental values during the whole process of combustion, (b) experimental values and model predictions during char combustion.

Although the model predicts relatively well the levels of the SSR efficiency as well as the influence of temperature and particle size, the differences between model predictions and experimentally obtained data are in some cases significant. This may be especially noticed in the case of combustion in the laboratory oven. Apart from the significant non-uniformity of the investigated coals [26], the possible reason for these differences may also be found in the simplifications adopted in the model, especially concerning the  $\text{CaSO}_4$  decomposition.

Hardly any experimental data on SSR could be found in the literature, with sufficient necessary supplementary data, that could be used for comparison with the model. Model predictions are compared with the available literature data [6,7] in Fig. 7. It may be seen that the agreement is better for the data of Yeh et al. [7], which is a consequence of the fact that these results were obtained for the batch combustion experiments, as considered by the model. For the data of

Fuertes et al. [6], which apply to the case of steady-state FBC combustion of coal, the measured values of the  $\eta_{\text{SO}_2}$  are higher than the model predictions. This is a result of the prolonged residence time of the ash remaining in the bed and thus the prolonged time for sulfation, which is not taken into account by the model.

With the aim of testing the model in greater detail, especially in relation to the kinetics of the process, the model predictions were compared with the measured  $\text{SO}_2$  concentrations monitored above the bed surface during the batch combustion experiments in the FBC reactor. In Fig. 8a it may be seen that a substantial part of the sulfur evolves during devolatilization and that the concentrations of  $\text{SO}_2$  are significantly higher than during char combustion. Since the evolution of  $\text{SO}_2$  during devolatilization is taken into account in the model by Eq. (1), the comparison between the experimental and model predicted  $\text{SO}_2$  concentrations was done only during char combustion, Fig. 8b. It may be seen that the model can adequately predict the evolution of  $\text{SO}_2$  during char combustion in the case of two coals with quite different sulfur content and Ca/S molar ratio (Table 1).

The typical spatial and temporal changes of the CaO conversion and  $\text{SO}_2$  concentration are shown in Fig. 9. Initially, only the CaO in outer layers ( $r/R_{\text{Ch}} \approx 1$ ) contribute to the SSR. As combustion proceeds, the combustion front moves inward and the  $\text{SO}_2$  concentration increases inside the char particle due to which the CaO conversion gradually progresses towards the char particle center. The final local CaO conversion (at the end of combustion) differs along the char particle radius, decreasing towards the particle center.

## 6. Conclusion

The results of experimental investigations and modeling of the phenomena of sulfur self-retention (SSR) during combustion of coal, by the coal ash itself, is presented in this work. The obtained experimental data give sufficient evidence that practically no SSR occurs during devolatilization. In the presented model, the transformations of sulfur forms during devolatilization are taken into account by a correlation whose derivation is based on theoretical considerations. A quite good agreement was obtained between the calculated and experimentally obtained values of the amount of sulfur that remains in the char, after devolatilization.

A novel approach has been applied for modeling the SSR process during char combustion, closely related to the grain model used for the  $\text{SO}_2$  retention by limestone as a sorbent. It is assumed that SSR is a result of the reaction between  $\text{SO}_2$  and the active CaO in the form of uniformly distributed micro-grains in char. An unreacted shrinking core model is adopted for the reactions between the CaO micro-grains and  $\text{SO}_2$ , taking into account ionic diffusion through the product layer formed on the CaO micro-grains. The decomposition of the formed  $\text{CaSO}_4$  at higher temperatures is taken into account by a reaction whose kinetics is of the Arrhenius type.

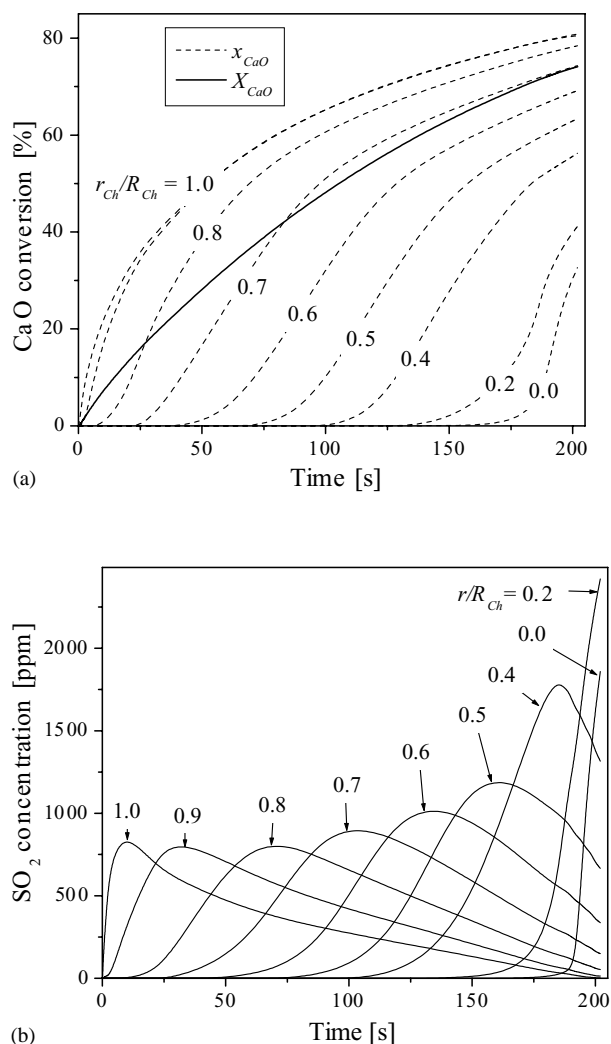


Fig. 9. Model predictions of spatial and temporal changes of CaO conversion (a) and  $\text{SO}_2$  concentration (b) inside a char particle during combustion.

The comparison with the experimentally obtained values in an FBC reactor and in a laboratory oven, using the coals of different rank, content of sulfur forms and molar Ca/S ratio, has shown that the model can adequately predict the kinetics of the process, the levels of the obtained values of SSR efficiencies, as well as the influence of temperature, coal particle size and the surrounding conditions. Besides simulating the dynamic behavior of the coal particle in relation to the sulfur self-retention, the developed model may be incorporated either directly in combustor models for estimation of SO<sub>2</sub> emissions without sorbent addition or used as an integral part of sulfur capture submodels in the case of sorbent addition.

### Acknowledgements

This work was supported by the Serbian Ministry for Science, Technology and Development under Projects No. NP EE401-86B and ETR.6.02.0202.A. The authors would like to thank Prof. Cor van den Bleek for his suggestions and advice, which supported our orientation to the investigations of sulfur retention and helped us to overcome some initial obstacles and misunderstandings in experimental research.

### References

- [1] S. Oka, Research and development of the fluidized bed combustion technology, Scientific review, *Sci. Eng. Ser.* 16 (1996) 53–73.
- [2] S. Oka, M. Ilic, D. Dakic, B. Grubor, Single coal particle behavior in fluidized bed combustion: recent results achieved in Vinca Institute, in: Proceedings of the ASME-ZSITS International Thermal Science Seminar, Bled, Slovenia, 2000, pp. 83–92.
- [3] B. Arsic, S. Oka, M. Radovanovic, Characterization of Yugoslav limestones in a fluidized bed reactor, in: Proceedings of the Fourth International Conference on Fluidized Bed Combustion, London, UK, 1989, pp. I/171–I/179.
- [4] R. Puff, J.-C. Kita, J.F. Large, A. Feugier, Self-desulfuration of high sulfur high ash Provence coal by the Cerchar F.B.C. process, in: Proceedings of the First International FBC and Applied Technology Symposium, Beijing, China, 1983, pp. 22–42.
- [5] A.P. Raymant, Sulfur capture by coal ash and freeboard processes during fluidized bed combustion, in: Proceedings of the 10th International Conference on Fluidized Bed Combustion, ASME, San Francisco, USA, 1989, pp. 597–602.
- [6] A.B. Fuertes, V. Artos, J.J. Pis, G. Marban, J.M. Palacios, Sulphur retention by ash during fluidized bed combustion of bituminous coals, *Fuel* 71 (1992) 507–511.
- [7] A.T. Yeh, Y.Y. Lee, W.E. Genetti, Sulfur retention by mineral matter in lignite during fluidized bed combustion, in: Proceedings of the Ninth International Conference on Fluidized Bed Combustion, ASME, Boston, USA, 1987, pp. 345–352.
- [8] B. Grubor, V. Manovic, B. Arsic, Influence of combustion conditions and coal characteristics on self-retention of SO<sub>2</sub> by ash itself, in: Proceedings of the Mediterranean Combustion Symposium, Antalya, Turkey, 1999, pp. 866–877.
- [9] M. Hartman, R.W. Coughlin, Reaction of sulfur dioxide with limestone and the grain model, *AIChE J.* 22 (3) (1976) 490–498.
- [10] G.J. Zijlma, A.W. Gerritsen, C.M. van den Bleek, SO<sub>2</sub> retention in fluidized bed combustors, modelling and influence of oxygen, in: Proceedings of the 15th International Conference on Fluidized Bed Combustion, ASME, Savannah, USA, 1999, on CD-ROM, No. FBC99-0167.
- [11] S.K. Mahuli, R. Agnihotri, R. Jadhav, S. Chauk, L.-S. Fan, Combined calcination, sintering and sulfation model for CaCO<sub>3</sub>–SO<sub>2</sub> reaction, *AIChE J.* 45 (2) (1999) 367–382.
- [12] A. Attar, Chemistry, thermodynamics and kinetics of reactions of sulphur in coal–gas reactions: a review, *Fuel* 57 (1978) 201–211.
- [13] G. Gryglewicz, Sulfur transformations during pyrolysis of a high sulfur Polish coking coal, *Fuel* 74 (3) (1995) 356–361.
- [14] J. Yperman, D. Franco, J. Mullens, L.C. Van Poucke, G. Gryglewicz, S. Jasienco, Determination of sulfur groups in pyrolysed low-rank coal by atmospheric-pressure TPR, *Fuel* 74 (9) (1995) 1261–1266.
- [15] I.I. Maes, G. Gryglewicz, H. Machnikowska, J. Yperman, D.V. Franco, J. Mullens, L.C. Van Poucke, Rank dependence of organic sulfur functionalities in coal, *Fuel* 76 (5) (1997) 391–396.
- [16] W.H. Calkins, The chemical forms of sulfur in coal: a review, *Fuel* 73 (4) (1994) 475–484.
- [17] W.H. Calkins, Investigation of organic sulfur-containing structures in coal by flash pyrolysis experiments, *Ener. Fuels* 1 (1) (1987) 59–64.
- [18] W.H. Calkins, R.J. Torres-Ordóñez, B. Jung, M.L. Gorbaty, G.N. George, S.R. Kelemen, Comparison of pyrolytic and X-ray spectroscopic methods for determining organic sulfur species in coal, *Ener. Fuels* 6 (4) (1992) 411–413.
- [19] F. Garcia-Labiano, E. Hampartsoumian, A. Williams, Determination of sulfur release and its kinetics in rapid pyrolysis of coal, *Fuel* 74 (7) (1995) 1072–1079.
- [20] F. Garcia-Labiano, J. Adanez, E. Hampartsoumian, A. Williams, Sulfur release during the devolatilization of large coal particles, *Fuel* 75 (5) (1996) 585–590.
- [21] A. Attar, F. Dupuis, The rate and the fundamental mechanisms of the reaction of hydrogen sulfide with the basic minerals in coal, *Ind. Eng. Chem. Process. Des. Dev.* 18 (4) (1979) 607–618.
- [22] V. Manovic, Influence of combustion conditions and coal characteristics on sulfur retention in ash, Master's Thesis, Chemistry Faculty, University in Belgrade, 2000 (in Serbian).
- [23] G. Gryglewicz, Effectiveness of high temperature pyrolysis in sulfur removal from coal, *Fuel Process. Technol.* 46 (1996) 217–226.
- [24] D. Uzun, S. Ozdogan, Correlations for the sulfur contents of Turkish coals exposed to ashing and devolatilization conditions at 750 and 950 °C, *Fuel* 77 (14) (1998) 1599–1604.
- [25] C. Chen, T. Kojima, Modeling of sulfur retention by limestone in coal briquette, *Fuel Process. Technol.* 53 (1997) 49–67.
- [26] B. Grubor, V. Manovic, Influence of non-uniformity of coal and distribution of active calcium on sulfur self-retention by ash—a case study of lignite Kolubara, *Ener. Fuels* 16 (4) (2002) 951–955.
- [27] C. Sheng, M. Xu, J. Zhang, Y. Xu, Comparison of sulphur retention by coal ash in different types of combustors, *Fuel Process. Technol.* 64 (2000) 1–11.
- [28] C. Sheng, J. Zhang, Y. Xu, Retention of sulphur by ashes from Chinese coals, in: Proceedings of the International Conference on Ash Behavior Control in Energy Conversion Systems, Pacifico Yokohama, Japan, 1998, pp. 86–93.
- [29] E. Raask, Mineral Impurities in Coal Combustion, Hemisphere Publishing, Washington, USA, 1985, p. 37.
- [30] V.R. Gray, Retention of sulphur by laboratory-prepared ash from low-rank coal, *Fuel* 65 (1986) 1618–1619.
- [31] R.E. Conn, T.E. Taylor, J. Tang, Evaluation on inherent sulfur capture from low-rank coals in circulating fluidized beds, in: Proceedings of the 12th International Conference on Fluidized Bed Combustion, ASME, San Diego, USA, 1993, pp. 273–281.
- [32] D. Allen, A.N. Hayhurst, Reaction between gaseous sulfur dioxide and solid calcium oxide. Mechanism and kinetics, *J. Chem. Soc., Faraday Trans.* 92 (7) (1996) 1227–1238.
- [33] E.J. Anthony, D.L. Granatstein, Sulphation phenomena in fluidized bed combustion systems, *Prog. Ener. Comb. Sci.* 27 (2001) 215–236.
- [34] J.C. Schouten, C.M. van den Bleek, The influence of oxygen-stoichiometry on desulfurization during FBC: a simple SURE modeling approach, *Chem. Eng. Sci.* 43 (8) (1988) 2051–2059.

- [35] J. Adanez, P. Gayan, L.F. de Diego, Modelling and simulation of the sulphur retention in circulating fluidized bed combustors, *Chem. Eng. Sci.* 51 (11) (1996) 3077–3082.
- [36] X. Li, Z. Luo, M. Ni, K. Cen, Modeling sulfur retention in circulating fluidized bed combustors, *Chem. Eng. Sci.* 50 (14) (1995) 2235–2242.
- [37] R. Korbee, E.H.P. Wolff, C.M. van den Bleek, A general approach to FBC Sulfur retention modeling, in: Proceedings of the 11th International Conference on Fluidized Bed Combustion, ASME, Montreal, Canada, 1991, pp. 907–916.
- [38] D.W. Marsh, D.L. Ulrichson, Rate and diffusional study of the reaction of calcium oxide with sulfur dioxide, *Chem. Eng. Sci.* 40 (3) (1985) 423–433.
- [39] R.H. Borgwardt, K.R. Bruce, J. Blake, An investigation of product-layer diffusivity for CaO sulfation, *Ind. Eng. Chem. Res.* 26 (1987) 1993–1998.
- [40] A. Lyngfelt, B. Leckner, SO<sub>2</sub> capture in fluidised-bed boilers: re-emission of SO<sub>2</sub> due to reduction of CaSO<sub>4</sub>, *Chem. Eng. Sci.* 44 (2) (1989) 207–213.
- [41] M. Hartman, O. Trnka, Influence of temperature on the reactivity of limestone particles with sulfur dioxide, *Chem. Eng. Sci.* 35 (1980) 1189–1194.
- [42] D. Uzun, S. Ozdogan, Correlations for the combustible sulfur contents of Turkish coals from sulfur forms and CaO analyses, *Fuel* 76 (11) (1997) 995–997.
- [43] M. Ilic, B. Grubor, V. Manovic, Sulfur retention by ash during coal combustion. I. A model of char particle combustion, *J. Serb. Chem. Soc.* 68 (2) (2003) 137–145.
- [44] M. Ilic, S. Oka, B. Grubor, Analysis of the dynamic behavior of a burning porous char particle, *Therm. Sci.* 2 (2) (1998) 61–73.
- [45] C. Hsia, G.R. St. Pierre, K. Raghunathan, L.-S. Fan, Diffusion through CaSO<sub>4</sub> formed during the reaction of CaO with SO<sub>2</sub> and O<sub>2</sub>, *AIChE J.* 39 (4) (1993) 698–703.
- [46] C. Hsia, G.R. St. Pierre, L.-S. Fan, Isotope study on diffusion in CaSO<sub>4</sub> formed during sorbent–flue–gas reaction, *AIChE J.* 41 (10) (1995) 2337–2340.
- [47] I.W. Smith, The intrinsic reactivity of carbons to oxygen, *Fuel* 57 (7) (1978) 409–414.
- [48] J. Scholer, Ein gesamtmodell für dampferzeugeranlangen mit zirkulierender wirbelschichtfeuerung, Ph.D. Thesis, Siegen University, Germany, 1992.
- [49] S.V. Patankar, Numerical Heat Transfer and Fluid Flow, Hemisphere Publishing Corporation, Washington, 1980.
- [50] S.K. Bhatia, D.D. Perlmutter, The effect of pore structure on fluid–solid reactions: application to the SO<sub>2</sub>-lime reaction, *AIChE J.* 27 (2) (1981) 226–234.
- [51] L.M. Diaz-Bossio, S.E. Squier, A.H. Pulsifer, Reductive decomposition of calcium sulfate utilizing carbon monoxide and hydrogen, *Chem. Eng. Sci.* 40 (3) (1985) 319–324.